PhD Discussion

Out-of-equilibrium dynamics in round-trip and dissipation protocols

Francesco Tarantelli

`francesco.tarantelli@phd.unipi.it`

University of Pisa and INFN

Supervisor: Prof. E.Vicari

17^{th} January

Introduction

- We address out-of-equilibrium dynamics of many-body systems subject to round-trip and dissipation protocols across quantum phase transitions;
- We perform quenched and Kibble-Zurek(KZ) protocols which develop dynamic scaling behavior at both the transitions obtained from a Renormalization Group(RG) framework;
- While classical and quantum models, belonging to the same universality class, show similar dynamic scaling frameworks, substantial differences emerge in the round-trip evolution;
- In the dissipation case, the Liouvillian gap plays a central role in the large-time regime.

Phase transitions and Critical phenomena

Many systems undergo a phase transition driven by a control parameter whose variation changes the phase of the system.

The order parameter assumes different values in each of the two phases and it shows a non-analytic behavior approaching the transition point.

We distinguish the transitions in two types:

- **first-order transitions** (FOT) where in the infinite volume limit the order parameter is discontinuous across the transition point;
- **continuous transitions** (CT) in which in the same limit a diverging length scale, characterizing the physical correlations, determines the non-analytical behavior of the order parameter.

Phase transitions and Critical phenomena

Classical Ising model

Ordered (broken) phase

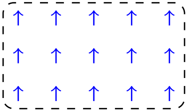

Disordered (symmetric) phase

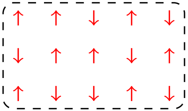

As example, we take the classical Ising model in which:

$$H = -J \sum_{\langle i,\, j \rangle} S_i \cdot S_j - h \cdot \sum_i S_i \qquad , \tag{1}$$

$$Z = \sum_{\{S_i\}} e^{-H/T} \qquad , \tag{2}$$

where $S_i = \pm 1$ and $i,\, j$ indicate the sites of a d-dimensional lattice.

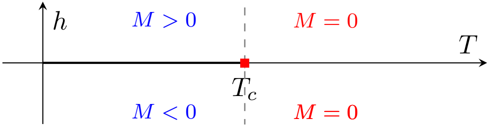

Phase transitions and Critical phenomena

Power-laws

The CTs are characterized by power-law behavior:

- the correlation length ξ defined as

$$\lim_{|i-j|\to\infty} \langle S_i \cdot S_j \rangle \sim e^{-|i-j|/\xi},$$

  scales as $\xi \sim |t|^{-\nu}$, $t = T/T_c - 1$;
- the order parameter M: $M \sim |t|^{\beta}$;
- the susceptibility $\chi = \sum_i \langle S_i \cdot S_j \rangle$: $\chi \sim |t|^{-\gamma}$;

where the parameters ν, β, and γ are called critical exponents.

Close to the critical point, i.e. $t \to 0$, the correlation length diverges to ∞.

Phase transitions and Critical phenomena

Renormalization group (RG)

Close to critical point, the many-body system shows an universal critical behavior dependent only by few global properties:

- the space dimensionality d,
- the nature and the symmetry of the order parameter,
- symmetry-breaking pattern.

These features are encoded in the renormalization group (RG) theory in which:

- we have a RG flow in the Hamiltonian space,
- the critical points are described by the fixed points of the theory,
- only a few perturbations are relevant, the corresponding positive eigenvalues are related to the critical exponents.

Quantum Transitions

Quantum phase transitions are driven by the variation of the Hamiltonian parameters which determine the non-analytic behavior of the ground state.

In the large-volume limit, the continuous quantum transitions (CQT) are characterized by:

- a diverging correlation length:

$$\xi \sim |\bar{g}|^{-\nu} \; ; \tag{3}$$

- a lowest energy gap Δ which vanishes:

$$\Delta \sim \xi^{-z} \sim |\bar{g}|^{z\,\nu} \; ; \tag{4}$$

where $\bar{g} = g - g_c$ is an Hamiltonian parameter which drives the quantum transition and z is the dynamic critical exponent.

Quantum Transitions

Example - Quantum Ising model

As a paradigmatic model for quantum transitions, we consider the quantum Ising model whose Hamiltonian is given by:

$$\hat{H}_{\mathrm{Is}} = -\sum_{x=1}^{L-1} \hat{\sigma}_x^{(1)} \hat{\sigma}_{x+1}^{(1)} - g \sum_{x=1}^{L} \hat{\sigma}_x^{(3)} \ , \tag{5}$$

where $\sigma_x^{(j)}$ are the Pauli matrices on the x^{th} site of the chain and L is the system size.

The system undergoes a quantum transitions at $g_c = 1$, between paramagnetic and ordered phases.

Kitaev Model

Kitaev Hamiltonian mapped into a spin-$1/2$ XY chain, by a Jordan-Wigner transformation (OBC): $\hat{c} \longrightarrow \hat{\sigma}$

$$\hat{H}_K^{(\mathrm{ABC})} = -\sum_{x=1}^{L}\left[\left(\hat{c}_x^\dagger\,\hat{c}_{x+1} + \hat{c}_{x+1}^\dagger\,\hat{c}_x\right) + \delta\left(\hat{c}_x\,\hat{c}_{x+1} + \hat{c}_{x+1}^\dagger\,\hat{c}_x^\dagger\right)\right] - \sum_{x=1}^{L}\mu\,\hat{c}_x^\dagger\,\hat{c}_x\ ; \quad (6)$$

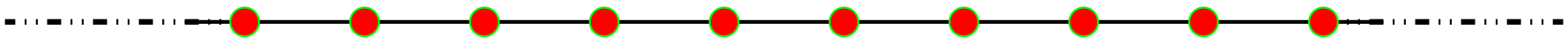

Continuous Transition point:

$$\mu_c = -2 \qquad \text{and} \qquad \delta = 1 \text{ fixed}\ ;$$

RG dimensions:

$$w = \mu - \mu_c \longrightarrow y_w = 1 \qquad \hat{c}_x\,,\ \hat{c}_x^\dagger \longrightarrow y_c = 1/2 \qquad \text{dynamic exp} : z = 1\ .$$

Finite Size Scaling (FSS) at the equilibrium

Kitaev model

At the critical point, the ground state $|0\rangle\langle 0|$ correlation function:

$$G_c(x,y,t) = \langle 0|\hat{c}_x^\dagger \hat{c}_y + \hat{c}_y^\dagger \hat{c}_x|0\rangle \ , \tag{7}$$

satisfies for $L \to \infty$ and using RG theory:

$$G_c(x,y,w) = b^{-2y_c}\,\mathcal{G}_c\left(x/b, y/b, w\, b^{y_\mu}\right) \ , \tag{8}$$

where $y_\mu = 1\,,\ y_c = 1/2$ are the RG dimensions of, respectively, the parameter μ and the fermionic operator $\hat{c}_x$ and $\hat{c}_x^\dagger$.

If the system size L is finite $\Longrightarrow$ in the FSS limit, i.e. when we keep the ratio ξ/L fixed for $L \to \infty$; in other words, when wee fix $b = L$, we have:

$$G_c(x,y,w;L) = L^{-1}\left[\mathcal{G}_c\left(X,Y,\kappa\right) + O(L^{-1})\right] \ , \tag{9}$$

$$X \equiv x/L\,, \qquad Y \equiv y/L\,, \qquad \kappa = w\,L^{y_\mu} \ . \tag{10}$$

Round - Trip

FT, E. Vicari PR B **105**, 235124

FT, S. Scopa PR B **108**, 104316

Kibble Zurek(KZ) Protocol

(i) Start at the equilibrium state (classical) and at the ground state $|\Psi(t = t_i)\rangle \equiv |\Psi(w_i < 0)\rangle$ (quantum);

(ii) quantum case:

$$\frac{d\,|\Psi(t)\rangle}{dt} = -i\hat{H}[w(t)]\,|\Psi(t)\rangle \;\; ;$$

(ii) classical one:

Metropolis algorithm;

$$\Downarrow$$

$$w(t) = t/t_s \;;$$

from $w_i < 0$ to $w_f > 0$, where t_s is the time scale of the slow variations of w.

(iii) Then, for $t > t_f$, $w(t)$ decreases with the same t_s, from $w_f > 0$ to the original value $wi < 0$, closing the cycle.

Observables

Classical Ising model

$$M(t) = \frac{1}{L^2} \sum_i \langle S_i \rangle_t \ ; \tag{11}$$

$$G(t, \boldsymbol{x}, \boldsymbol{y}) \equiv \langle s_{\boldsymbol{x}} \, s_{\boldsymbol{y}} \rangle_t \, . \tag{12}$$

Quantum models

Adiabaticity function:

$$A(t) = \Big| \langle \Psi_0[w(t)] | \Psi(t) \rangle \Big| ; \tag{13}$$

Kitaev:

$$C(x, t) \equiv \langle \Psi(t) | \, c_j^\dagger c_{j+x} + c_{j+x}^\dagger c_j \, | \Psi(t) \rangle \ .$$

The Round-Trip

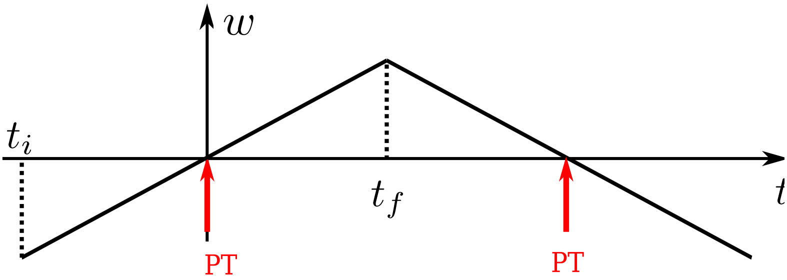

Figure 1: Round-trip Protocol: the intersection with the x-axis corresponds to the phase transition (PT) point.

Dynamic scaling framework for the round-trip

The asymptotic dynamic FSS behavior is obtained by taking $t_s \to \infty$ and $L \to \infty$:

$$\begin{aligned} K &= w(t) L^{y_w} \,, \qquad & \Upsilon &= t_s / L^{\zeta} \,, \\ \Theta_i &= w_i \, t_s^{1-\kappa} \,, \qquad & \Theta &= w(t) \, t_s^{1-\kappa} = t / t_s^{\kappa} \,, \end{aligned} \tag{14}$$

where

$$\zeta = y_w + z \,, \qquad \kappa = z/\zeta \,, \qquad 1 - \kappa = y_w / \zeta \,. \tag{15}$$

with $w_f = -w_i = w_\star$, we have:

$$\Upsilon = t_s / L^{\zeta} \,, \quad \Theta = w(t) \, t_s^{1-\kappa} \,, \quad \Theta_\star = w_\star \, t_s^{1-\kappa} \,. \tag{16}$$

Numerical results - Classical Ising

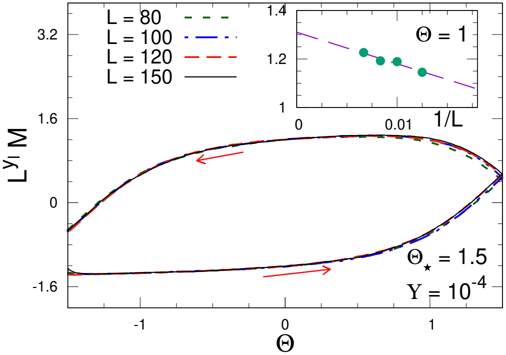

Figure 2:
$M^{(a/b)}(t, t_s, w_\star, L) \approx L^{-y_l}\mathcal{M}_i(\Upsilon, \Theta, \Theta_\star)$
$\Upsilon = 10^{-4}$, fixed $\Theta_\star = 1.5$ and plotted versus $\Theta = w(t)t_s^{1-\kappa}$.

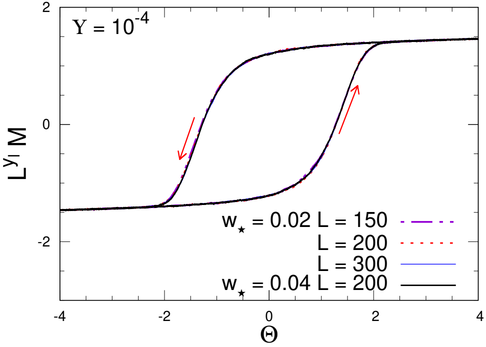

Figure 3: Thermalized classical state for fixed $\Upsilon = 10^{-4}$, and fixed $w_\star = 0.02$ and $w_\star = 0.04$.

No returned convergence as in the classical one

Numerical results - Kitaev chain

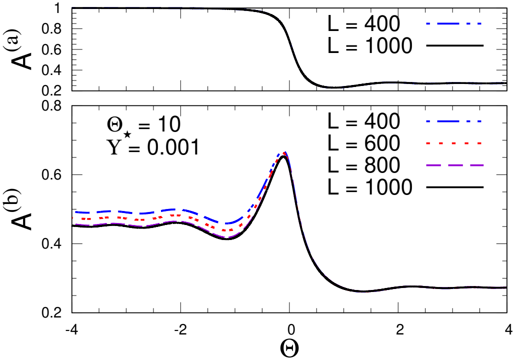

Figure 4: $A^{(a/b)}(t, t_s, w_\star, L) \approx \mathcal{A}^{(a/b)}(\Upsilon, \Theta, \Theta_\star)$; Finite $\Theta_\star = 10$ at fixed $\Upsilon = t_s/L^\zeta = 0.001$ and $\Theta_\star = w_\star L^{1-\kappa} = 10$, for outward and return.

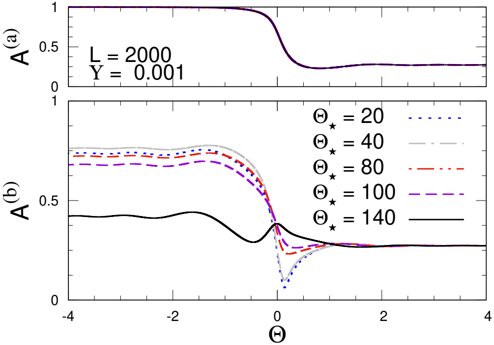

Figure 5: At $L = 2000$ and $\Upsilon = 0.001$ for the outward (top) and return (bottom), versus Θ, for various $\Theta_\star$.

The limit $\Theta_\star \to \infty$

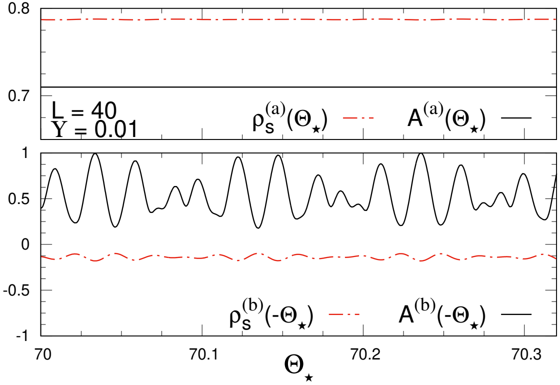

Figure 6: **Kitaev** - Fixed $L = 40$, $\Upsilon = 0.01$ versus $\Theta_\star$, close to $\Theta_\star = 70$. The top plot shows the values at $\Theta = \Theta_\star$, while the bottom at $\Theta = -\Theta_\star$, with the particle density $\rho_s = \langle\Psi(t)|\, c_x^\dagger c_x \,|\Psi(t)\rangle - \rho_{\text{critical-gs}}$.

Two-Level Model: $H_{2\ell}(t) = -\beta(t)\sigma^{(3)} + \frac{\Delta}{2}\sigma^{(1)}$

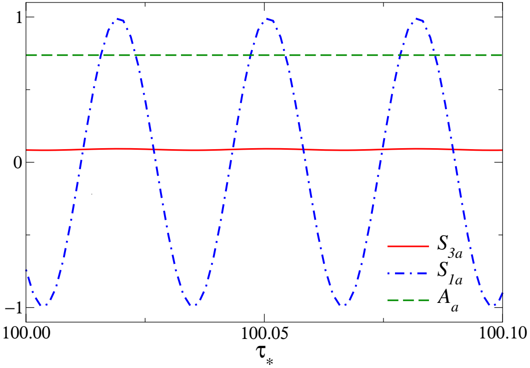

Figure 7: Dependence on $\tau_\star \equiv t_\star/\sqrt{t_s}$ at the end of the first dynamic branch for $\upsilon = 1$, and $\tau_\star \approx 100$.

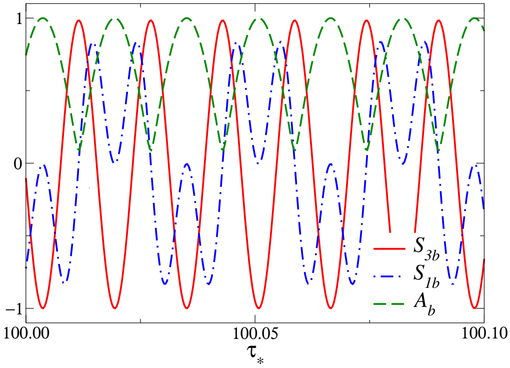

Figure 8: Dependence on $\tau_\star$ at the end of round-trip protocol for $\upsilon = t_s\Delta^2 = 1$, and $\tau_\star \approx 100$.

First Order Quantum Transition (FOQT)

$$\hat{H}(h_\perp, h_\parallel) = -J\sum_{j=1}^{L-1} \hat{\sigma}_j^{(3)}\hat{\sigma}_{j+1}^{(3)} - \sum_{j=1}^{L}(h_\perp\hat{\sigma}_j^{(1)} + h_\parallel\hat{\sigma}_j^{(3)}). \tag{17}$$

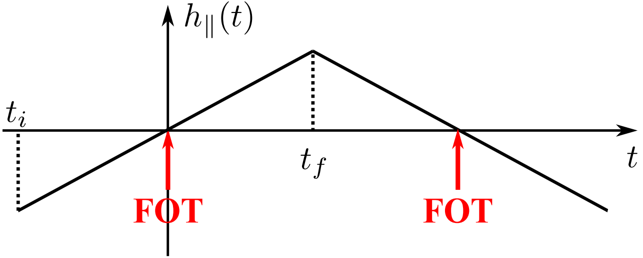

Figure 9: FOQT Round-trip Protocol where we keep $h_\perp$ fixed and $h_\parallel(t) = t/t_s$.

Out-Of-Equilibrium FSS at FOQT

Degeneracy of the 2 lowest energy levels for $L \to \infty$ approaching the FOQT point $\longrightarrow$ Two-levels model

We formulate the OFSS regime as the limit $L \to \infty$, $u = t_s L^{-1} M_0^{-1} \to \infty$.

The time-dependent expectation values of local observables are proportional to quasi-universal OFSS functions of the variables:

$$\tau = \frac{t}{\sqrt{u}} \ , \tag{18}$$

$$\upsilon = u \ \Delta^2(h_\perp, L) \ . \tag{19}$$

Validity of our scaling hypothesis

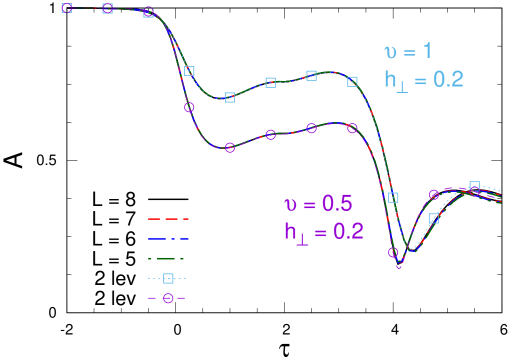

Figure 10: OFSS of the adiabaticity function in $A(h_\perp, t, t_s, L) \sim \mathcal{F}_A(\tau, \upsilon)$ shown as a function of the rescaled time τ during a round-trip protocol with $|\tau_i| = \tau_f = 2$ (FOTs at $\tau = 0, 4$).

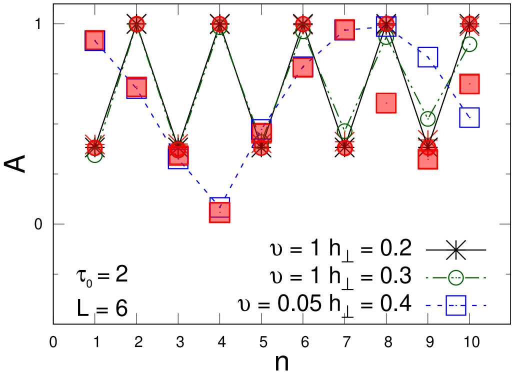

Figure 11: Stroboscopic evolution of A as function of n (corresponding to times $t = t_0(4n - 1)$) at fixed $L = 6$, $\tau_0 = 2$

Effective description in the OFSS regime

Emergence of an effective two-level description which involves the lowest two states near the FOT.

With this effective description, we reduce the driving protocol to a series of LZS and we determine an analytical expression of the OFSS functions:

$$\mathcal{F}_A(\tau,\upsilon) = e^{-\frac{\pi\upsilon}{32}} \Bigg| \sqrt{\frac{1}{2} + \frac{|\tau|}{\sqrt{4\tau^2+\upsilon}}}\,\mathscr{D}_{\frac{iu}{8}}\big(\sqrt{2}e^{i\frac{3\pi}{4}}\tau\big) - \frac{\sqrt{\upsilon}e^{-\frac{i\pi}{4}}}{2\sqrt{2}} \sqrt{\frac{1}{2} - \frac{|\tau|}{\sqrt{4\tau^2+\upsilon}}}\,\mathscr{D}_{-1+\frac{iu}{8}}\big(\sqrt{2}e^{i\frac{3\pi}{4}}\tau\big) \Bigg| \tag{20}$$

Breakdown of the effective description

Corrections to the scaling behavior are expected when:

$$\tau \gtrsim O(t_{KZ}) \qquad \text{with} \qquad t_{KZ} = \sqrt{u}\ .$$

Dissipation

A. Franchi, FT PR B **108**, 094114
FT, E.Vicari PR B **108**, 035128

Open quantum systems

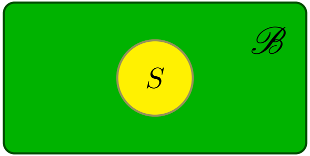

Any empirical test involves a non-negligible influences on the quantum object S being measured.

In the approximation of weak couplings, we model the interaction with a Markovian bath $\mathscr{B}$ by the Lindblad master equation for the density matrix ρ of the system S :

$$\frac{\partial\rho}{\partial t} = -i\Big[H,\,\rho\Big] + \mathbb{D}\;. \tag{21}$$

Open quantum systems

If b indicates the parts of the open system S in contact with an independent bath, the dissipator $\mathbb{D}$ corresponds to the sum:

$$\mathbb{D} = \sum_b w_b \, \mathbb{D}_b \ , \qquad \mathbb{D}_b = L_b \rho L_b^\dagger - \frac{1}{2}\left(\rho L_b^\dagger L_b + L_b^\dagger L_b \rho\right) \ ,$$

where the Lindblad operator L_b describes the interaction of the system part b with its independent environment $\mathscr{B}_b$ and w_b tunes the strength of the associated dissipative mechanism.

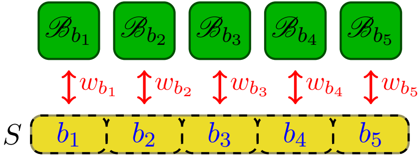

Sunburst geometry

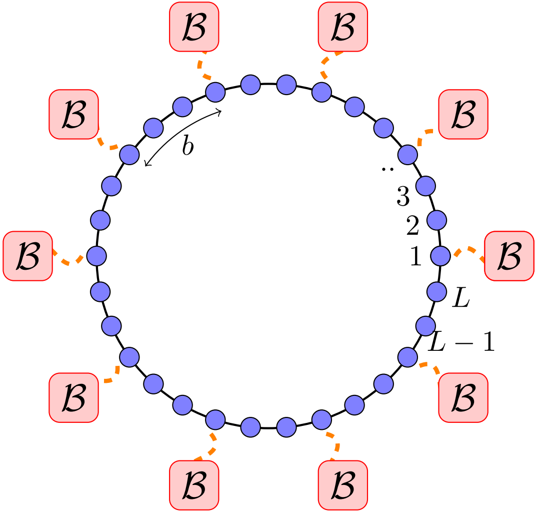

Liouvillian gap

$$\widetilde{\mathcal{L}}[\widetilde{\rho}_i] = \lambda_i \widetilde{\rho}_i \ , \qquad \lambda_i \in \mathbb{C} \ ; \tag{22}$$

$$\rho_{ij} \left|i\right\rangle \left\langle j\right| \longrightarrow \widetilde{\rho}_{ij} \left|i\right\rangle \left|j\right\rangle \ . \tag{23}$$

$$\widetilde{\mathcal{L}} = -i\big(\hat{H} \otimes \hat{\mathbb{I}} - \hat{\mathbb{I}} \otimes \hat{H}^t\big) + w \sum_{x\in\mathcal{I}} \hat{L}_x \otimes \hat{L}_x^* \tag{24}$$

$$-\frac{w}{2} \sum_{x\in\mathcal{I}} \big(\hat{L}_x^\dagger \hat{L}_x \otimes \hat{\mathbb{I}} + \hat{\mathbb{I}} \otimes \hat{L}_x^t \hat{L}_x^*\big) \ . \tag{25}$$

$$\Delta_\lambda = -\max_i \mathrm{Re}\lambda_i \ . \tag{26}$$

Interplay between local and homogeneous dissipation

The number of the external baths:

$$n \equiv L/b \; ; \tag{27}$$

b fixed $\longrightarrow$ local dissipation with $\Delta_\lambda \sim L^{-1} f(\mu, wL) \qquad L \to \infty$;

n fixed $\longrightarrow$ homogeneous dissipation with $\Delta_\lambda \sim L^{-3} \tilde{f}(\mu, w) \qquad L \to \infty$.

Liouvillian gap b fixed

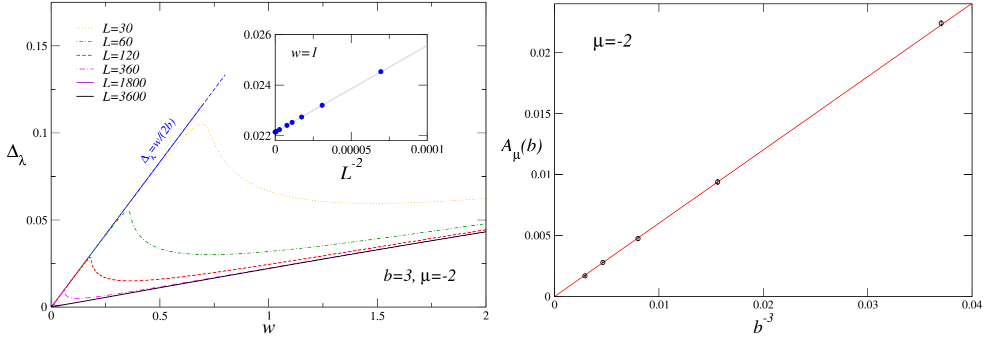

Figure 13: Liouvillian gap Δ_λ in terms of the dissipation coupling w for $b = 3$ and fixed $\mu = -2$.

$$\Delta_\lambda(w, b) = A_\mu(b) w\,, \quad A_\mu(b) = \frac{C_\mu}{b^3}\,, \quad w > w_*\,, \tag{28}$$

Liouvillian gap b fixed

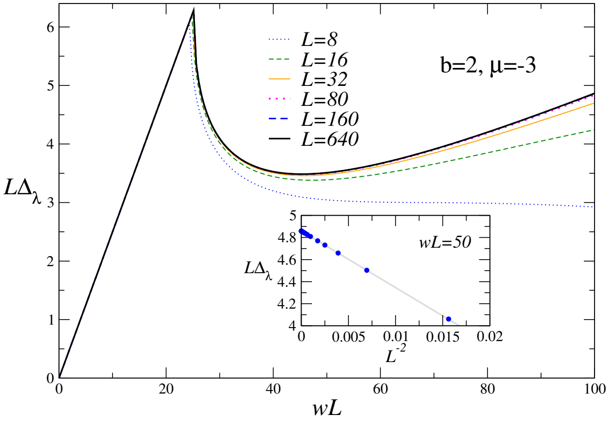

Liouvillian gap n fixed

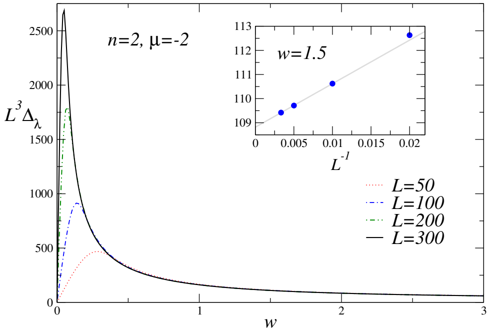

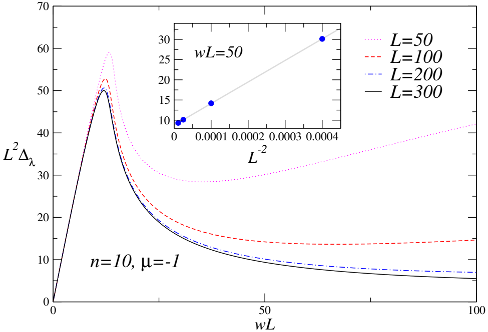

Dynamic Finite Size Scaling

The correlation function as observable:

$$C(x,y,t) \equiv \mathrm{Tr}[\rho(t)(\hat{c}_x^\dagger \hat{c}_y + \hat{c}_y^\dagger \hat{c}_x)]\,, \tag{29}$$

$$P(x,y,t) \equiv \mathrm{Tr}[\rho(t)(\hat{c}_x^\dagger \hat{c}_y^\dagger + \hat{c}_y \hat{c}_x)]\,. \tag{30}$$

The scaling parameters are set:

$$M_{i/f} = (\mu_{i/f} - \mu_c)L^{y_\mu} \qquad y_\mu = 1\ ; \tag{31}$$

$$\Theta = tL^{-z}\,,\ z = 1 \text{ for } t \sim L\ ; \qquad \Theta = t/\Delta_\lambda \text{ for } t \sim L^3\ ; \tag{32}$$

$$\gamma_b = \frac{wL^z}{b}\ . \tag{33}$$

The Scaling Laws can be expressed:

$$C(x,y,t) \approx L^{-2y_c}\mathcal{C}(M_i, M_f, \{X_i\}, \Theta, \gamma_b)\ ,$$

$$P(x,y,t) \approx L^{-2y_c}\mathcal{P}(M_i, M_f, \{X_i\}, \Theta, \gamma_b)\,.$$

Numerical Results

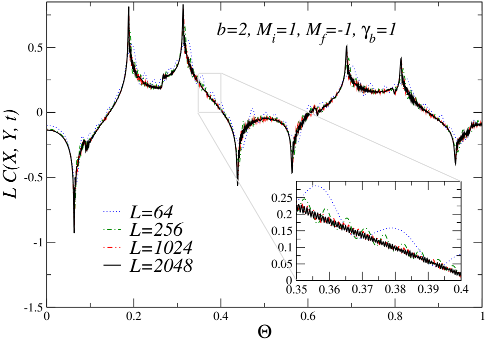

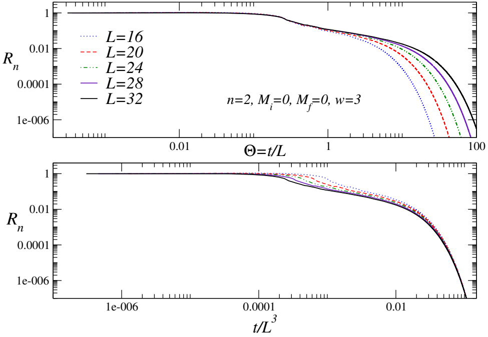

We introduce the RG invariant quantity R_n defined as

$$R_n = \frac{N(t) - N_{\text{asy}}}{N(0) - N_{\text{asy}}}\,, \tag{34}$$

where $N(t) = \sum_x^L \langle \hat{c}_x^\dagger \hat{c}_x(t) \rangle$ and $N_{\text{asy}} = \lim_{t\to\infty} N(t)$.

Conclusions

In the round-trip model:

- Analogy of the scaling behaviors at classical and quantum transitions is only partially extended to round-trip KZ protocols. Substantial differences emerge:
  1. classical systems develop scaling hysteresis-like scenarios,
  2. in quantum systems, the persistence of oscillating relative phases make the return way extremely sensitive to the parameters of the protocol;
- Even in the simple two-level quantum model, we have a similar behavior.

In the dissipation scenario:

- When we keep b fixed, the gap Δ_λ is always finite and depends linearly on the dissipation strength w ;
- Two different regimes:
  1. In the small w region, the gap is given by $\Delta_\lambda = w/(2b)$;
  2. At large w and sufficiently large b, $\Delta_\lambda = wC_\mu/b^3$ controls the gap in the large-size limit and the dynamic FSS.